

EFFECTS OF SYNTHETIC ESTROGENS, (*R,R*)-(+)-, (*S,S*)-(-)-, *dl*- AND *meso*-HEXESTROL STEREOISOMERS ON MICROTUBULE ASSEMBLY*

YUMIKO SAKAKIBARA,† KIYOSHI HASEGAWA,† TAIKO ODA,† HAZIME SAITÔ,‡ MASAHIKO KODAMA,‡ AIKO HIRATA,§ MICHIO MATSUHASHI§ and YOSHIHIRO SATO†||

† Biochemistry Division, Kyoritsu College of Pharmacy, Shibakoen 1-chome, Minato-ku, Tokyo 105;
‡ Biophysics Division, National Cancer Center Research Institute, Tsukiji 5-chome, Chuo-ku, Tokyo 104; and § Institute of Applied Microbiology, The University of Tokyo, Yayoi 1-chome, Bunkyo-ku, Tokyo 113, Japan

(Received 15 December 1988; accepted 7 August 1989)

Abstract—We previously reported on the inhibition of microtubule polymerization and the formation of ribbon structures by synthetic estrogens [Sato *et al.*, *J Biochem* **101**: 1247-1252, 1987]. The present investigation aimed to analyse these effects *in vitro* on stereochemical point of view, using hexestrol isomers (*R,R*)-(+)-hexestrol, (*S,S*)-(-)-hexestrol and *meso*-hexestrol and *dl*-hexestrol. Among hexestrols, *dl*-hexestrol showed the highest activity in ribbon formation from microtubule proteins at 100 μ M. On the other hand, *meso*-hexestrol was distinguished from others by inhibition of microtubule assembly and formation of a large amount of aggregates from purified tubulin in the presence of MgCl₂ and DMSO. These results were discussed with physico-chemical properties of hexestrols, e.g. absolute configurations as well as circular dichroism spectra and solid state carbon-13 nuclear magnetic resonance spectra.

A synthetic estrogen, diethylstilbestrol (DES),¶ is not only clinically effective in chemotherapy of breast and prostate cancers [1, 2] but also carcinogenic in experimental animals [3] and in humans [4, 5]. DES, which induces neoplastic transformation in cultured cells [6], is rather an exceptional carcinogen without appreciable mutagenic activities [6-8]. The carcinogenicity could be best explained in terms of aneuploidy [9] due to disturbed assembly of microtubule proteins [10-12]. In the present situation, however, it is difficult to completely rule out other important contributions, e.g. metabolic activation [13], DNA binding [14], radical formation [15] or DNA breaks [16]. Further, another synthetic estrogen, *meso*-hexestrol, is shown to induce renal carcinoma in castrated male hamster as DES or 17 β -estradiol [17].

In a preceding paper [18], we showed that *meso*- and *dl*-hexestrol not only have an inhibitory effect on microtubule assembly from microtubule proteins but also accumulate twisted ribbon structures *in vitro*. The formation of the twisted ribbon structures in the presence of *meso*- or *dl*-hexestrol has also

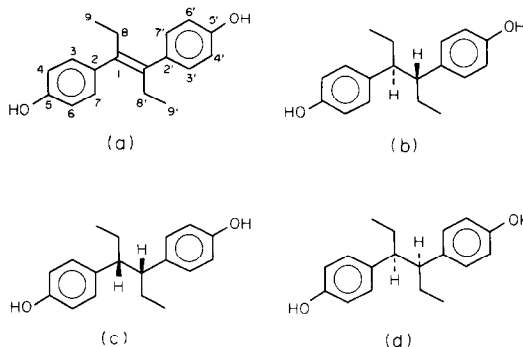


Fig. 1. Structures of hexestrol stereoisomers: (a) diethylstilbestrol, (b) *meso*-hexestrol[(*R,S*)-hexestrol], (c) (*R,R*)-(+)-hexestrol and (d) (*S,S*)-(-)-hexestrol.

* This study was supported in part by Grant-in-Aid for Scientific Research from the Ministry of Education, Science and Culture of Japan (No. 61571064), by The Science Research Promotion Fund from Japan Private School Promotion Foundation (1986), and by Haraguchi Memorial Cancer Research Fund (T.O.).

|| To whom correspondence should be addressed.

¶ Abbreviations: DES, diethylstilbestrol; DMSO, dimethyl sulfoxide; MES, 2-(morpholino)ethanesulfonic acid; EGTA, ethyleneglycol-bis(2-aminoethylether)-*N,N,N',N'*-tetraacetic acid; EDTA, ethylenediamine tetraacetate; DMF, *N,N*-dimethylformamide; MAPs, microtubule-associated proteins; CD, circular dichroism; CP-MAS, cross polarization-magic angle spinning.

recently been reported by Chaudoreille *et al.* [19]. Although *dl*-hexestrol was used in our previous experiment, it is indispensable to investigate the respective activity of its stereochemical enantiomers, (*R,R*)-(+)- and (*S,S*)-(+)-hexestrols, to clarify the relationship between effects on microtubules and structures of hexestrols.

In this report, we described the effects of (*R,R*)-(+)-hexestrol, (*S,S*)-(-)-hexestrol, *meso*-hexestrol and *dl*-hexestrol (Fig. 1) in a system of microtubule proteins and of purified tubulin. In the former system, all the hexestrols inhibited the normal microtubule assembly, accompanied by the formation of ribbon structures. In the latter system supplemented with DMSO, (*R,R*)-(+)-, (*S,S*)-(-)- and *dl*-hexestrols did not inhibit microtubule formation whereas *meso*-hexestrol caused formation of aggregates.

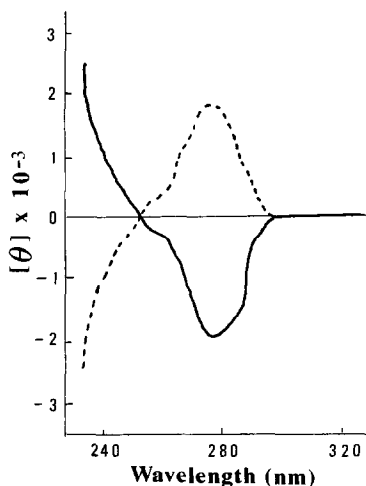


Fig. 2. CD curves of (*R,R*)-(+)- and (*S,S*)-(-)-hexestrols. (—) (*R,R*)-(+)-hexestrol; (----) (*S,S*)-(-)-hexestrol.

These results were discussed in connection with the physico-chemical data of each hexestrol stereoisomers.

MATERIALS AND METHODS

Preparation of microtubule proteins and tubulin. Microtubule proteins were prepared from porcine brains by two cycles of temperature-dependent assembly–disassembly by the method of Shelanski *et al.* [20] with some modifications [21]. The microtubule proteins were stored at -70° for later use. Tubulin was purified from two-cycle microtubule proteins by phosphocellulose method described by Kumagai and Nishida [22].

Assembly assay. The effect of the test compounds on microtubule proteins or purified tubulin at 37° was determined by turbidity measurement [23] at 400 nm using a UVIDEC 430B double-beam spectrometer equipped with a thermostatically controlled cell holder. Microtubule proteins were adjusted to a concentration of 3.0 mg protein/ml in 5 mM MES,

0.5 mM $MgSO_4$, 1 mM EGTA, 50 mM KCl and 1 mM GTP (pH 6.5), and used as 1 ml aliquots for measurement. Purified tubulin was prepared at a concentration of 1.8 mg protein/ml in 0.1 M MES, 10 mM $MgCl_2$, 0.1 mM EDTA, 2 mM EGTA, 1 mM 2-mercaptoethanol and 0.5 mM GTP (pH 6.8). One ml aliquots of tubulin were incubated after addition of 100 μ l DMSO. Each test compound was dissolved in a 1:1 mixture of DMSO and DMF [24] and this solution was added to the protein solution at a volume ratio of 2%.

Electron microscopy. Samples were fixed by addition of 9 volumes of the buffer for assembly containing 1% glutaraldehyde. A few minutes later, carbon-coated collodion 150 mesh copper grids were placed on the drops of fixed sample solution and rinsed with the same buffer. The samples were then negatively stained with 1% uranyl acetate solution and air-dried. Specimens were examined on a JEOL 200 CX electron microscope at 100 kV.

Protein concentration. Concentrations of microtubule proteins and purified tubulin were determined by the method of Lowry *et al.* [25] using serum albumin as the standard.

Apparatus for structural determination. Optical rotations were measured on a JASCO DIP-SL automatic polarimeter with a cell of 10-cm light path length, and CD spectra were taken in a 0.5-mm cell at room temperature (24 – 25°) in chloroform on JASCO J-20 recording spectropolarimeter. High-resolution solid state ^{13}C NMR spectra (at 75.46 MHz) were recorded on a Bruker CXP-300 spectrometer equipped with an accessory for cross polarization-magic angle spinning (CP-MAS) as described previously [26].

Materials. *meso*-Hexestrol was obtained from Wako Pure Chemical Industries, Ltd (Osaka, Japan). *dl*-Hexestrol (m.p. 132°) was prepared [27] by catalytic hydrogenation of DES (Tokyo Chemical Industry Co., Ltd, Tokyo, Japan) over 5% palladium–charcoal in ethyl acetate at ambient pressure, and purified through silica gel chromatography. *dl*-Hexestrol was treated with 3 α -bromocamphor-9 π -sulfonyl chloride to give its corresponding sulfonyl ester. Recrystallization of the ester from acetone–ethanol afforded (+)-hexestrol-3 α -bromocamphor-9 π -sulfonyl ester as crystals, m.p. 188° , $[\alpha]_D^{25} + 73.3^{\circ}$

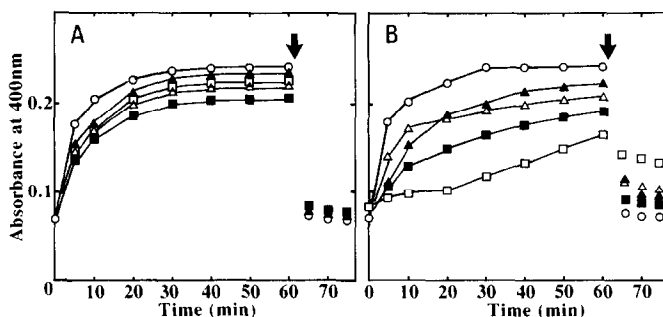


Fig. 3. Turbidimetric analysis of assembly-inhibition by hexestrol isomers at 37° . Test compounds were added to microtubule proteins (3 mg/ml) at 0 min. Final drug concentration was 50 μ M (A) or 100 μ M (B). Arrow indicates cold treatment. (O) control; (Δ) (*R,R*)-(+)-hexestrol; (\blacktriangle) (*S,S*)-(-)-hexestrol; (\square) *dl*-hexestrol; (\blacksquare) *meso*-hexestrol.

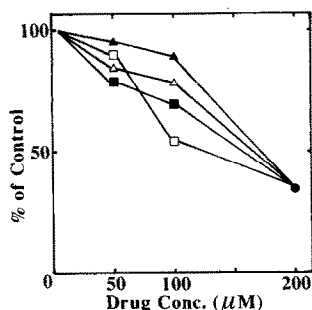


Fig. 4. The extent of microtubule polymerization by hexestrol enantiomers: concentration dependence. After 60 min of polymerization, the absorbance at each hexestrol concentration was determined. The vertical is shown as % of control. (Δ) (*R,R*)-(+)-hexestrol; (\blacktriangle) (*S,S*)-(-)-hexestrol; (\square) *dl*-hexestrol; (\blacksquare) *meso*-hexestrol.

83°, $[\alpha]_D^{23} - 36.0^\circ$ ($c = 1.64$, CHCl_3). Analysis calculated for $\text{C}_{18}\text{H}_{22}\text{O}_2$: C, 79.96; H, 8.20. Found: C, 80.28; H, 8.10. CD ($c = 1.65$ mg/ml, CHCl_3) $[\theta]^{25}(\text{nm})$: 0(295), +1900(277) (positive maximum), 0(254), -5060(230). (+)-Hexestrol di-*p*-bromobenzoate (m.p. 127–128°) was obtained for X-ray crystallographic analysis by treatment of (+)-hexestrol with *p*-bromobenzoyl chloride in pyridine. ATP and GTP were obtained from Yamasa Shoyu Co., Ltd (Choshi, Japan), and the materials for electron microscopy were obtained from Nissin EM Co., Ltd (Tokyo, Japan). All other reagents were obtained from Wako Pure Chemical Industries, Ltd.

RESULTS AND DISCUSSION

Stereochemistry of (+)-hexestrol

(+)-Hexestrol has been proved chemically as a (*R,R*) configuration [29, 30] which was recently confirmed by X-ray diffraction analysis of (+)-hexestrol

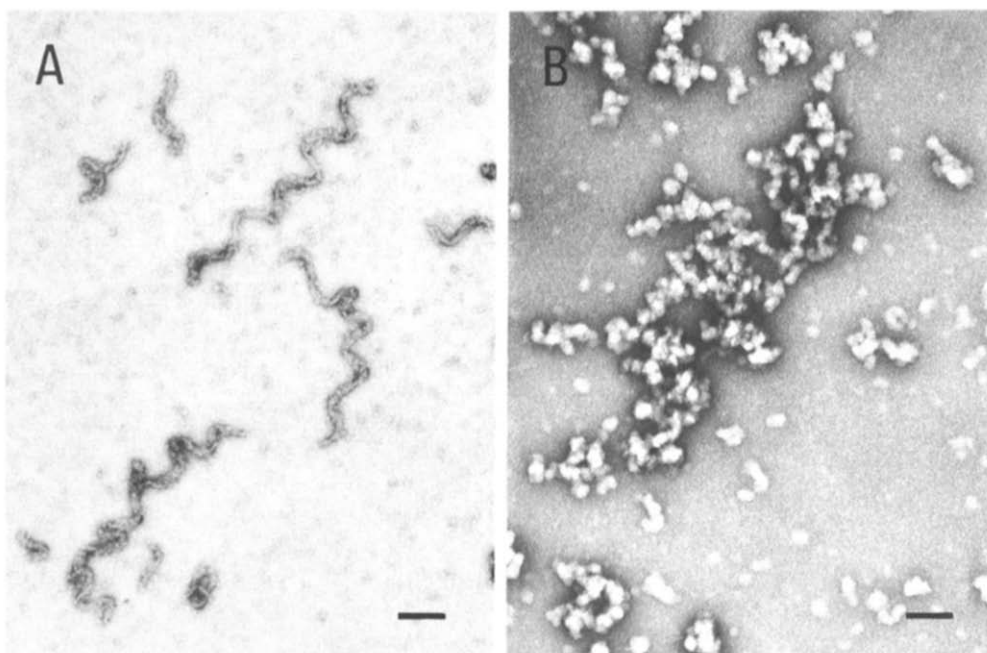


Fig. 5. Electron micrographs of microtubule proteins incubated at 37° for 20 min in the presence of *dl*-hexestrol. (A) Only ribbons were observed at concentration of 200 μM, but (B) after cold treatment, only small particles were observed. Bar, 100 nm.

($c = 0.12$, CHCl_3). Alkaline hydrolysis and silica gel chromatography gave free (+)-hexestrol [28]. Recrystallization from methylene chloride gave (+)-hexestrol as colourless needles, m.p. 82–83°, $[\alpha]_D^{23} + 38.0^\circ$ ($c = 0.25$, CHCl_3). Analysis calculated for $\text{C}_{18}\text{H}_{22}\text{O}_2$: C, 79.96; H, 8.20. Found: C, 79.95; H, 8.05. CD ($c = 0.80$ mg/ml, CHCl_3) $[\theta]^{25}(\text{nm})$: 0(295), -2030(277) (negative maximum), 0(254), +5080(230). The ethanol soluble fraction which was obtained from the first recrystallization of the sulfonyl ester was concentrated and alkaline hydrolysis and silica gel chromatography gave free (-)-hexestrol. Recrystallization from methylene chloride gave (-)-hexestrol as colorless needles, m.p. 82–

di-*p*-bromobenzoate (Itai *et al.*, unpublished results). Consequently, (-)-hexestrol should be a (*S,S*) stereoisomer. These compounds exhibited CD spectra which indicated that (*R,R*)-(+)-hexestrol has a negative Cotton effect and the (*S,S*)-(-)-isomer shows the positive one (Fig. 2). The crystal structure of *dl*-hexestrol has been reported to be different from that of DES [31–33].

Effects of hexestrol stereoisomers on microtubule proteins

We examined the effects of (*R,R*)-(+)-hexestrol, (*S,S*)-(-)-hexestrol, *dl*-hexestrol and *meso*-hexestrol [(*R,S*)-hexestrol] on microtubule polymerization.

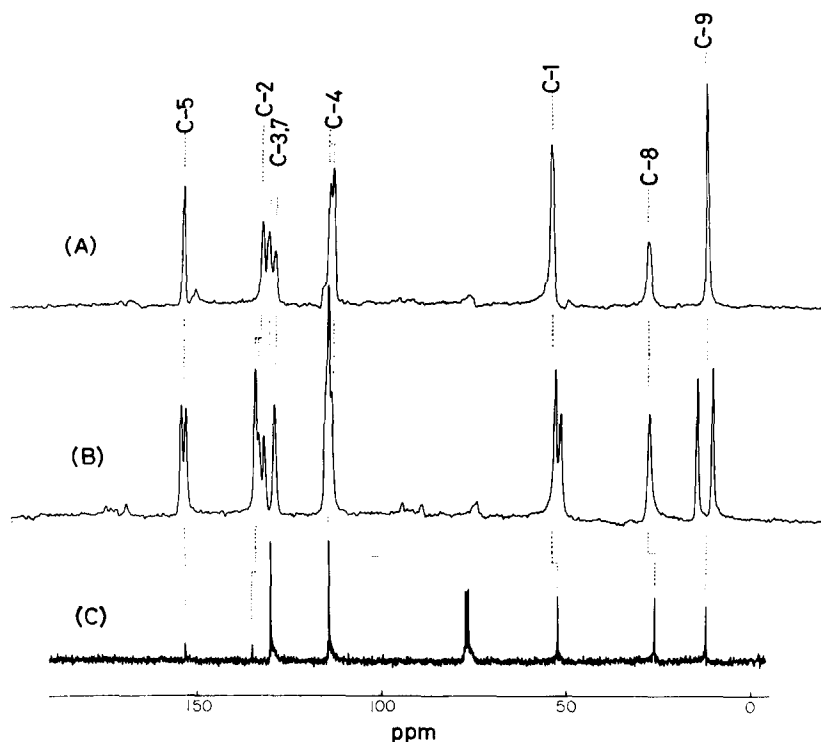


Fig. 6. ^{13}C CP-MAS NMR spectra (75.46 MHz) of (A) *(R,R)*-(+)-hexestrol and (B) *dl*-hexestrol in the solid state together with (C) the ^{13}C NMR spectrum of *dl*-hexestrol recorded in deuteriochloroform solution.

Table 1. ^{13}C chemical shifts of *dl*- and (+)-hexestrol in the solid state (ppm from TMS)*

Compound	C-1	C-2	C-3/C-7	C-4/C-6	C-5	C-8	C-9
<i>meso</i> -Hexestrol†	54.8	137.6	132.4	118.6	152.9	27.8	12.8
	53.9	135.8	125.8	117.3			
<i>dl</i> -Hexestrol	53.2	133.8	131.6	114.6	153.7	27.9	15.2
	51.7	132.9	128.7	114.0	152.3		11.1
				113.2			
	(52.4)	(135.1)	(130.0)	(114.3)	(153.2)	(26.1)	(12.3)
(+)-Hexestrol	54.2	131.9	130.1	113.5	152.8	27.9	12.5
			128.6	112.7			

* Data in parentheses are from deuteriochloroform solution.

† Taken from Ref. 26.

The inhibitory activities of these compounds detected by turbidity measurement depended on the concentration used. At 50 μM , the activities decreased in the following order: *meso*-hexestrol > *(R,R)*-(+)-hexestrol > *dl*-hexestrol > *(S,S)*-(-)-hexestrol (Fig. 3A). This order, however, was disturbed at 100 μM , and *dl*-hexestrol showed the highest inhibitory activity among the four isomers (Fig. 3B). Here, it should be noticed that 100 μM *dl*-hexestrol is composed of 50 μM *(R,R)*-(+)-hexestrol and 50 μM *(S,S)*-(-)-hexestrol. At 200 μM , increase of turbidity was almost equally suppressed by the above compounds, and there appears to be a tendency for the inhibitory activity of hexestrols to saturate (data not shown). Figure 4 showed the relation of turbidity

values by microtubule polymerization and concentrations of hexestrol stereoisomers, at 50, 100 and 200 μM . From this figure, it was clearly shown that at below 100 μM *(R,R)*-(+)- and *(S,S)*-(-)-hexestrols exhibit low activity and those activities were weaker than that of *meso*-hexestrol. However, interestingly the coexistence of the enantiomers as the racemate strengthened the activity at 100 μM as compared with that of only one of the enantiomers.

At 100 μM , *meso*-hexestrol induced ribbon-microtubules and ribbons, and *dl*-hexestrol formed only ribbon structures as described in the previous paper [18]. At 200 μM , all compounds were found active in the formation of ribbons which were transformed into small particles after a cold treatment (Fig. 5).

These results may contradict that of Chaudoreille *et al.* [19], who reported that twisted ribbon structures formed in the presence of dienestrol were stable in the cold treatment. On the other hand, when microtubule proteins were incubated at 4° in the presence of 200 μM of *meso*-hexestrol, the ribbon structure was not formed.

Effects of hexestrol isomers on purified tubulin

As reported in our previous paper, formation of ribbon structures from tubulin induced by hexestrols depended on the presence of MAPs [18]. In a system consisting of purified tubulin, MgCl_2 and DMSO, *meso*-hexestrol inhibited microtubule assembly forming aggregates at concentrations higher than 100 μM [18]. In contrast, its isomers, (*R,R*)-(+)-, (*S,S*)-(-)- and *dl*-hexestrols did not inhibit microtubule formation in the same condition. Both aggregates induced by *meso*-hexestrol and microtubules formed in the presence of other isomers were transformed into tangles by cold treatment. Thus, the activity of *meso*-hexestrol on tubulin assembly seemed to be different from other isomers.

Effects of molecular configurations on the activities of hexestrols

We previously reported that (+)-griseofulvin was much more active in inhibiting microtubule assembly than (-)-griseofulvin [34]. In the present investigation, (*R,R*)-(+)-hexestrol showed higher extent of inhibition than (*S,S*)-(-)-hexestrol at 50 μM , but almost the same extent of inhibition at concentrations higher than 100 μM . Although *meso*-hexestrol was prominent in inhibition of microtubule assembly, *dl*-hexestrol also exhibited an extraordinary activity at 100 μM exceeding any other isomers. It is worth investigating why the racemate is more active than its enantiomers alone.

Recently, we have reported that ^{13}C NMR signals of *meso*-hexestrol in the solid state are split into a pair of peaks, in contrast to observations in solution [35], because the conformation of the two phenol moieties in the solid state is not always identical [26]. In the present work we found that the ^{13}C NMR spectrum of *dl*-hexestrol in the solid state gives rise to considerably different spectral pattern from that of (*R,R*)-(+)-hexestrol (Fig. 6 and Table 1), although their spectra are identical in solution. Similar crystalline modification of racemic mixtures was noted in optically pure and *dl*-tartaric acids [36]. As a result, the C-5, C-2 and C-4 peaks in aromatic moieties as well as C-1 and C-9 peaks of *dl*-hexestrol are split into a pair of doublet patterns. It appears that conformation of *dl*-hexestrol is not identical with that of (*R,R*)-(+)-hexestrol as judged from the displacements of ^{13}C NMR peaks. In particular, the C-9 methyl ^{13}C signals which are sensitive [37] to intermolecular packing are significantly different from the corresponding peak of (*R,R*)-(+)-hexestrol. There is also a possibility that torsion angle about the C1-C2 and the manner of hydrogen bonding at C5-OH are different among two enantiomers and racemate (see Fig. 6A and B). In particular, the conformational change of *dl*-hexestrol from that of (*R,R*)-(+)- or (*S,S*)-(-)-hexestrol is obviously caused by the presence of specific interaction

between (*R,R*)-(+)- and (*S,S*)-(-)-enantiomers. In support of this view, melting point (m.p. 132°) of the racemate is higher than that (m.p. 82–83°) of the (*R,R*)-(+)- or (*S,S*)-(-)-enantiomer. This means that the racemate pair, (*R,R*)-(+)-(*S,S*)-(-), is more stable than pairs of (*R,R*)-(+)-(*R,R*)-(+)- and (*S,S*)-(-)-(*S,S*)-(-) isomers. Such racemic pairs will be readily dissociated to give an isolated molecule in DMSO/DMF solution. Nevertheless, it is also conceivable that a racemate is again formed in aqueous media of sparing solubility and/or less hydrophilic environment at the site of binding to the protein. Thus, such a racemic mixture or *meso*-hexestrol could interact differently with the microtubule proteins. Such an explanation might be responsible for enhanced biological activity of a racemate over the (*R,R*)-(+)- or (*S,S*)-(-)-enantiomer. To confirm this we are planning the X-ray analysis of (*R,R*)-(+)-hexestrol itself.

Present observations along with our previous results [10, 18, 26] including "disruptive effect of DES on microtubules" will provide a basis for further study of enantiomers and corresponding racemate in *in vitro* protein-drug interactions.

Acknowledgement—We wish to express our thanks to Dr A. Itai, University of Tokyo, for X-ray crystallographic analysis. We are also grateful to Messrs K. Hayashi and K. Ishizuka for their technical assistance.

REFERENCES

- Kennedy BJ and Nathanson IT, Effects of intensive sex steroid hormone therapy in advanced breast cancer. *J Am Med Assoc* **152**: 1135–1141, 1953.
- Flocks RH, Marberger H, Bergley BJ and Prendergast LJ, Prostatic carcinoma: Treatment of advanced cases with intravenous diethylstilbestrol diphosphate. *J Urol* **74**: 549–551, 1955.
- Kirkman H and Bacon RL, Malignant renal tumors in male hamsters (*Cricetus auratus*) treated with estrogen. *Cancer Res* **10**: 122–123, 1950.
- Herbest MD, Ulfelder H and Poskanzer DC, Adenocarcinoma of the vagina: Association of maternal stilbestrol therapy with tumor appearance in young women. *N Engl J Med* **284**: 878–881, 1971.
- Krishna G, Corsini GU, Gillette J and Brodie BB, Biochemical mechanisms for hepatotoxicity produced by diethylstilbestrol. *Toxicol Appl Pharmacol* **23**: 794, 1972.
- Barrett JC, Wong A and McLachlan JA, Diethylstilbestrol induces neoplastic transformation without measurable gene mutation at two loci. *Science* **212**: 1402–1404, 1981.
- McCann J, Choi E, Yamasaki E and Ames BN, Detection of carcinogens as mutagens in the *Salmonella*/microsome test: Assay of 300 chemicals. *Proc Natl Acad Sci USA* **72**: 5135–5139, 1975.
- Glatt HR, Metzler M and Oesch F, Diethylstilbestrol and 11 derivatives: A mutagenicity study with *Salmonella typhimurium*. *Mutat Res* **67**: 113–121, 1979.
- Tsutsui T, Maizumi H, McLachlan JA and Barrett JC, Aneuploidy induction and cell transformation by diethylstilbestrol: A possible chromosomal mechanism in carcinogenesis. *Cancer Res* **43**: 3814–3821, 1983.
- Sato Y, Murai T, Tsumuraya M, Saitô H and Kodama M, Disruptive effect of diethylstilbestrol on microtubules. *Gann* **75**: 1046–1048, 1984.
- Sharp DC and Parry JM, Diethylstilbestrol: the binding

- and effects of diethylstilbestrol upon the polymerisation and depolymerisation of purified microtubule protein *in vitro*. *Carcinogenesis* **6**: 865–871, 1985.
12. Hartley-Asp B, Deinum J and Wallin M, Diethylstilbestrol induces metaphase arrest and inhibits microtubule assembly. *Mutat Res* **143**: 231–235, 1985.
 13. Metzler M, Studies on the mechanism of carcinogenicity of diethylstilbestrol: Role of metabolic activation. *Fd Cosmet Toxicol* **19**: 611–615, 1981.
 14. Blackburn GM, Thompson MH and King HWS, Binding of diethylstilbestrol to deoxyribonucleic acid by rat liver microsomal fractions *in vitro* and in mouse foetal cells in culture. *Biochem J* **158**: 643–646, 1976.
 15. Metzler M and McLachlan A, Peroxidase-mediated oxidation, a possible pathway for metabolic activation of diethylstilbestrol. *Biochem Biophys Res Commun* **85**: 874–884, 1978.
 16. Goldenberg GJ and Froese EK, Induction of DNA single- and double-strand breaks by diethylstilbestrol in murine L5178Y lymphoblasts *in vitro*. *Biochem Pharmacol* **34**: 771–776, 1985.
 17. Li TT, Li SA, Klicka JK, Parsons JA and Lam LK, Relative carcinogenic activity of various synthetic and natural estrogens in the Syrian hamster kidney. *Cancer Res* **43**: 5200–5204, 1983.
 18. Sato Y, Murai T, Oda T, Saitô H, Kodama M and Hirata A, Inhibition of microtubule polymerization by synthetic estrogens: Formation of a ribbon structure. *J Biochem* **101**: 1247–1252, 1987.
 19. Chaudoreille MM, Peyrot V, Braguer D and Crevat A, Interaction of some estrogenic drugs with tubulin. Formation of twisted ribbon structures. *Mol Pharmacol* **32**: 731–736, 1987.
 20. Shelanski ML, Gaskin F and Cantor CR, Microtubule assembly in the absence of added nucleotides. *Proc Natl Acad Sci USA* **70**: 765–768, 1973.
 21. Ishikawa M, Murofushi H and Sakai H, Bundling of microtubules *in vitro* by fodrin. *J Biochem* **94**: 1209–1217, 1983.
 22. Kumagai H and Nishida E, The interactions between calcium-dependent regulator protein of cyclic nucleotide phosphodiesterase and microtubule proteins: II. Association of calcium-dependent regulator protein with tubulin dimer. *J Biochem* **85**: 1267–1274, 1979.
 23. Gaskin F, Cantor CR and Shelanski ML, Turbidimetric studies of the *in vitro* assembly and disassembly of porcine neurotubules. *J Mol Biol* **89**: 737–758, 1974.
 24. Sato Y, Saito Y, Shiratori Y, Shoda S and Hosoi J, Structure-activity study of griseofulvin and its derivatives for the *in vitro* inhibition of microtubule polymerization and the *in vitro* depolymerization of microtubule. *Nippon Kagaku Kaishi* (in Japanese) 746–753, 1981.
 25. Lowry OH, Rosebrough NJ, Farr AL and Randall RJ, Protein measurement with the Folin phenol reagent. *J Biol Chem* **193**: 265–275, 1951.
 26. Saitô H, Yokoi M, Aida M, Kodama M, Oda T and Sato Y, ¹³C NMR spectra of para-substituted methoxybenzenes and phenols in the solid state: Examination of chemical shift non-equivalence in *ortho* and *meta* carbons related to non-equivalent electron distribution, and application to assignment of peaks in *meso*-hexestrol and its derivatives. *Magn Reson Chem* **26**: 155–161, 1988.
 27. Schwenk E, Papa D, Whitman B and Ginsberg HF, Reductions with nickel-aluminium alloy and aqueous alkali. IV. The carbon-carbon double bond. *J Org Chem* **9**: 175–177, 1944.
 28. Collins DJ and Hobbs JJ, Antioestrogenic and antifertility compounds: III. Enantiomers of (±)-hexestrol and its homologues. *Aust J Chem* **23**: 1605–1624, 1970.
 29. Inhoffen HH, Kopp D, Maric S, Bekurdt J and Selimoglu R, Untersuchungen an hochsubstituierten Äthylenen und Glykolen, X Zur Stereochemie der Hexoestrole. *Tetrahedron Lett* 999–1002, 1970.
 30. Collins DJ and Hobbs JJ, The absolute configuration of (+)-3,4-bis(*p*-hydroxyphenyl)hexane (hexestrol) and related compounds. *Aust J Chem* **27**: 1753–1758, 1974.
 31. Weeks CM, Pokrywiecki S and Duax WL, (±)-Hexestrol, analog of a synthetic estrogen. *Acta Cryst B* **29**: 1729–1731, 1973.
 32. Smiley IE and Rossmann MG, The crystal structure of αα'-diethylstilbene-4,4'-diol. *J Chem Soc, Chem Commun* 198, 1969.
 33. Weeks CM, Cooper A and Norton DA, The crystal and molecular structure of diethylstilbestrol. *Acta Cryst B* **26**: 429–433, 1970.
 34. Sato Y, Tezuka T, Oda T and Hosoi J, Viscometric and electron microscopic analysis of effects of griseofulvin and its derivatives on *in vitro* polymerization of microtubule proteins and depolymerization of microtubules. *J Pharm Dyn* **7**: 156–170, 1984.
 35. Oda T, Murai T and Sato Y, Carbon-13 nuclear magnetic resonance study of *meso*-hexestrol and its derivatives. *Chem Pharm Bull* **36**: 1534–1539, 1988.
 36. Hill HDW, Zens AP and Jacobus J, Solid-state NMR spectroscopy. Distinction of diastereomers and determination of optical purity. *J Am Chem Soc* **101**: 7090–7091, 1979.
 37. Saitô H, Tabeta R and Yokoi M, High-resolution ¹³C NMR study of free and metal-complexed ionophores in the solid state: Conformation and dynamics of the macrocyclic ring and the effect of intermolecular short contact of methyl groups on spin-lattice relaxation times and displacement of chemical shifts. *Magn Reson Chem* **26**: 775–786, 1988.